Bayesian redshift-space distortions correction from galaxy redshift surveys

Francisco-Shu Kitaura,[1][★] Metin Ata,[1] Raul E. Angulo,[2] Chia-Hsun Chuang,[3] Sergio Rodríguez-Torres,[3,4,5] Carlos Hernández Monteagudo,[2] Francisco Prada[3,4,6] and Gustavo Yepes[5]

[1]*Leibniz-Institut für Astrophysik Potsdam (AIP), An der Sternwarte 16, D-14482 Potsdam, Germany*
[2]*Centro de Estudios de Física del Cosmos de Aragón (CEFCA), Plaza San Juan, 1, planta 2, E-44001 Teruel, Spain,*
[3]*Instituto de Física Teórica, (UAM/CSIC), Universidad Autónoma de Madrid, Cantoblanco, E-28049 Madrid, Spain*
[4]*Campus of International Excellence UAM+CSIC, Cantoblanco, E-28049 Madrid, Spain*
[5]*Departamento de Física Teórica, Universidad Autónoma de Madrid, Cantoblanco, E-28049 Madrid, Spain*
[6]*Instituto de Astrofísica de Andalucía (CSIC), Glorieta de la Astronomía, E-18080 Granada, Spain*

ABSTRACT

We present a Bayesian reconstruction method which maps a galaxy distribution from redshift- to real-space inferring the distances of the individual galaxies. The method is based on sampling density fields assuming a lognormal prior with a likelihood modelling non-linear stochastic bias. Coherent redshift-space distortions are corrected in a Gibbs-sampling procedure by moving the galaxies from redshift- to real-space according to the peculiar motions derived from the recovered density field using linear theory. The virialized distortions are corrected by sampling candidate real-space positions along the line of sight, which are compatible with the bulk flow corrected redshift-space position adding a random dispersion term in high-density collapsed regions (defined by the eigenvalues of the Hessian). This approach presents an alternative method to estimate the distances to galaxies using the three-dimensional spatial information, and assuming isotropy. Hence the number of applications is very broad. In this work, we show the potential of this method to constrain the growth rate up to $k \sim 0.3\,h\,\mathrm{Mpc}^{-1}$. Furthermore it could be useful to correct for photometric redshift errors, and to obtain improved baryon acoustic oscillations (BAO) reconstructions.

Key words: methods: numerical – methods: observational – galaxies: general – cosmology: theory – large-scale structure of Universe.

1 INTRODUCTION

Galaxy redshift surveys produce the three-dimensional distribution of luminous sources tracing the underlying dark matter field. However, their inferred line-of-sight position is a combination of the so-called Hubble flow, i.e. their real distance, and their peculiar motion. The modifications produced by this effect are referred to as redshift-space distortions (RSD). Many astronomical studies are limited by these distortions, such as a proper environmental study (Nuza et al. 2014). Nevertheless, RSD can also be used to constrain the nature of gravity and cosmological parameters (see e.g. Berlind, Narayanan & Weinberg 2001; Zhang et al. 2007; Guzzo et al. 2008; Jain & Zhang 2008; Nesseris & Perivolaropoulos 2008; McDonald & Seljak 2009; Percival & White 2009; Song & Koyama

2009; Song & Percival 2009; White, Song & Percival 2009; Song et al. 2010, 2011; Zhao et al. 2010, for recent studies). The measurement of RSD have in fact become a common technique (Cole, Fisher & Weinberg 1995; Peacock et al. 2001; Percival et al. 2004; da Ângela et al. 2008; Guzzo et al. 2008; Okumura et al. 2008; Blake et al. 2011; Jennings, Baugh & Pascoli 2011; Kwan, Lewis & Linder 2012; Okumura, Seljak & Desjacques 2012; Reid et al. 2012; Samushia, Percival & Raccanelli 2012; Blake et al. 2013; de la Torre et al. 2013; Samushia et al. 2013, 2014; Zheng et al. 2013; Bel et al. 2014; Beutler et al. 2014; Okumura et al. 2014; Sánchez et al. 2014; Tojeiro et al. 2014). These studies are usually based on the large-scale anisotropic clustering displayed by the galaxy distribution in redshift space, although *N*-body-based models for fitting the data to smaller scales have been presented in Reid et al. (2014).

In this work, we use the full three-dimensional distribution of galaxies and correct in a statistical Bayesian way their individual positions according to a physical model describing the relation

★ E-mail: kitaura@aip.de

between the density and peculiar velocity fields which depends on the growth rate. This relation becomes more complex if one wants to correct for dispersed RSD as we will discuss below. The main finding of this work is that already very simple assumptions, such as a lognormal prior for the density field, a power-law galaxy bias, and linear theory to infer the peculiar motions with an adjustable smoothing scale, can yield accurate reconstructions of the real-space position of galaxies beyond the Kaiser factor.

In the following section, we will present our methodology and subsequently we will present the application on a mock galaxy catalogue. Finally, we will summarize our findings and present our conclusions.

2 METHOD

Our method essentially follows the algorithm (ARGO-code) proposed in Kitaura & Enßlin (2008) and Kitaura, Gallerani & Ferrara (2012a) by iteratively sampling the density and peculiar velocity fields within a Gibbs sampling process (for the pioneering iterative correction of linear RSD see Yahil et al. 1991):

$$\delta \curvearrowleft \mathcal{P}\left(\delta \mid N(\{r\}), \{b_{\mathrm{p}}\}, \mathbf{C}, w\right) , \tag{1}$$

$$\{r\} \curvearrowleft \mathcal{P}\left(\{r\} \mid \{s^{\mathrm{obs}}\}, \{v(\delta, f_{\Omega}, r_{\mathrm{S}}, \mathcal{H}, \{v_{\mathrm{p}}\})\}\right) . \tag{2}$$

In the first Gibbs-sampling step: δ is the dark matter overdensity field, $\mathcal{P}\left(\delta \mid N(\{r\}), \{b_{\mathrm{p}}\}, \mathbf{C}, w\right)$ the posterior distribution function of density fields given the number counts of galaxies in real space on a grid $N(\{r\})$, a covariance matrix $\mathbf{C} \equiv \langle \delta \delta^{\dagger} \rangle$ (the power-spectrum in Fourier space), a set of parameters describing galaxy bias $\{b_{\mathrm{p}}\}$, and a three-dimensional completeness w. In the second Gibbs-sampling step, we obtain the real-space position $\{r\}$ from the redshift-space position of galaxies and the sampled peculiar velocity fields $\{v\}$, which depend on the large scales, on the over-density field, the growth factor f_{Ω}, and a smoothing scale r_{S}; and in the non-linear regime additional information about the Hessian $\mathcal{H}$ and parameters describing the velocity of galaxies $\{v_{\mathrm{p}}\}$.

2.1 Density field reconstruction

We will restrict ourselves to a simple set of assumptions and demonstrate that they are sufficient for the scope set in this work, namely correct for RSD. The first Gibbs-sampling iteration assumes that the galaxies are in real space and applies a Hamiltonian sampling technique (Jasche & Kitaura 2010), to obtain the density field within the lognormal approximation with stochastic bias (Kitaura, Jasche & Metcalf 2010). In particular, we consider the negative binomial distribution function with non-linear bias, as introduced in Ata, Kitaura & Müller (2015). We note that the prior could be improved introducing higher order correlation functions (Kitaura 2012) or perturbation theory based methods (see e.g. Kitaura 2013). Nevertheless, we want to remain with simple models which require the least number of assumptions and parameters.

The deterministic non-linear bias we consider here is restricted to the following form: $\rho_{\mathrm{g}} = \gamma \rho_{\mathrm{M}}^{\alpha}$, with ρ_{g} being the expected number density of galaxies in a cell within a volume embedded in a mesh, ρ_{M} being the dark matter density on the same mesh, α being the power-law bias, and γ the proportionality factor dependent on the mean number density. Here we have neglected threshold bias, which would yield a more precise description in terms of higher order statistics (Kitaura, Yepes & Prada 2014; Kitaura et al. 2015).

We do not consider non-local bias, which will be introduced in a forthcoming publication.

2.2 Peculiar motion reconstruction

The redshift-space position of a galaxy s^{obs} is composed by its real-space position r and the coherent and dispersed components $v_r^{\mathrm{coh}}(r)$ and $v_r^{\sigma}(r)$, respectively: $s^{\mathrm{obs}} = r + v_r^{\mathrm{coh}}(r) + v_r^{\sigma}(r)$, with the subscript r denoting the projection along the line of sight. Let us discuss both redshift-space contributions separately below.

2.2.1 Coherent RSD

Coherent RSD are responsible for the squashing effect of galaxy clusters along the line of sight (see Hamilton 1998, for a review). This produces an enhancement of power on large scales, the so-called Kaiser (1987) factor.

For simplicity, we focus in this work on linear theory based on the density field (δ). We are aware that improvements could be found based on the linearized density field ($\log(1 + \delta)$), which we get for free in our formalism. However, it is also true that the logarithmic transformation introduces a constant offset which we do not want to consider here, as it was shown in Neyrinck, Szapudi & Szalay (2009) (for more general relations including linearizations see Kitaura et al. 2012b, and references therein). We simply consider a Gaussian smoothing (with radius r_{S}) of the overdensity field to optimize the velocity divergence to overdensity relation. For this component we do not assume any stochastic component, but directly move each galaxy from its redshift-space position s^{obs} to its coherent real-space position r_{coh}^{i} at iteration i, according to the coherent bulk flow motion $v_r^{\mathrm{coh},i}(r^{i-1})$ based on the real-space position from the previous iteration $i - 1$: $r_{\mathrm{coh}}^{i} = s^{\mathrm{obs}} - v_r^{\mathrm{coh},i}(r^{i-1})$, with $v_r \equiv (v \cdot \hat{r})\hat{r}/(Ha)$, where v is the full three-dimensional velocity field, $\hat{r}$ is the unit sight line vector, H the Hubble constant and a the scale factor.

2.2.2 Dispersed RSD

Further in the non-linear regime in deep gravitational wells, galaxy clusters are quasi-virialized, and produced so-called fingers-of-god which are elongated structures along the line of sight (Jackson 1972). This reduces the clustering towards small scales. A method aiming at correcting these effects needs thus to enhance the clustering of galaxies in clusters. We do so by first making sure that the galaxies come from collapsed regions in real space. To this end we demand that the real-space candidate positions along the line of sight come from cells in which all the eigenvalues of the Hessian are positive (Hahn et al. 2007) and above a certain overdensity threshold δ_{th}. This supposes another quantitative application of the cosmic web classification, in addition to the first of such kind presented in Zhao et al. (2015). For each real-space candidate position r_k, we sample the virialized motion component from a Gaussian with dispersion $\sigma(r_k) = \eta \rho_{\mathrm{M}}^{\epsilon}(r_k)(r)$: $v_r^{\sigma}(r_k) = \mathcal{G}\left(v_r^{\sigma}(r_k) \mid \sigma(r_k), \forall \lambda(\mathcal{H}(\delta) > 0)\right) \hat{r}$, with additional parameters η and ϵ (see Kitaura et al. 2014).

We can then find coherent real-space positions $r_{k\mathrm{coh}} = r_k + v_r^{\sigma}(r_k)$ and select the closest one in each iteration: $\min(|r_{\mathrm{coh}} - r_{k\mathrm{coh}}|)$. Additionally, to ensure that the clustering of clusters is enhanced we demand that the local density of the candidate's real-space position is larger or equal than in the previous iteration: $\delta(r_k)^i \geq \delta(r_k)^{i-1}$. We note that a similar approach was taken using the KIGEN-code

(Kitaura et al. 2012c; Kitaura 2013) to correct for fingers-of-god in a forward approach (see Heß, Kitaura & Gottlöber 2013).

3 APPLICATION TO MOCK DATA

We will focus in this work on mock galaxies constructed using the halo abundance matching technique based on the CMASS LRG sample (see Rodríguez-Torres et al. in preparation), and the Big-MultiDark (BIGMD) *N*-body simulation.

3.1 Reference galaxy catalogue

In particular, we performed a halo abundance matching using the redshift $z = 0.5763$ from one of the BIGMD simulations (see http://www.multidark.org/MultiDark/; Klypin et al. 2014), which was performed using the TREEPM *N*-body code GADGET-2 (Springel 2005) with 3840^3 particles and the volume of $(2.5\,h^{-1}\mathrm{Gpc})^3$, in a framework of Planck ΛCDM cosmology with $\{\Omega_\mathrm{m} = 0.307\,115, \Omega_\mathrm{b} = 0.048\,206, \sigma_8 = 0.8288, n_s = 0.96\}$, and the Hubble parameter $(H_0 \equiv 100\,h\,\mathrm{km\,s^{-1}Mpc^{-1}})$ given by $h = 0.6777$. We used the spherical overdensity (BDM) halo catalogue. The first step to generate the galaxy catalogue is to modify the maximum circular velocity ($V_{\max}$) of each objects adding a Gaussian noise $V_{\max}^{\mathrm{new}} = V_{\max}(1 + \mathcal{N}(0, \sigma_s))$ where $\mathcal{N}(0, \sigma_s)$ is a Gaussian random number with mean 0, and standard deviation σ_s. Then, we sorted all objects by $V_{\max}^{\mathrm{new}}$ and then, we selected objects starting from the one with larger $V_{\max}^{\mathrm{new}}$ and we continue until we get a number density of $3.29 \times 10^{-4}h^3\,\mathrm{Mpc^{-3}}$. Finally, we fit the clustering of the Baryon Oscillation Spectroscopic Survey (BOSS SDSS-III) CMASS sample using the scatter parameter σ_s. We consider for our study the catalogue in a sub-volume of $(1.25\,h^{-1}\,\mathrm{Gpc})^3$.

3.2 Reconstruction results

To avoid systematic effects in our study, we neglect incompleteness due to the survey geometry or the radial selection function, and neglect light-cone evolution effects. All these issues will be considered in a forthcoming work (Ata et al. in preparation). We compute the redshift-space position for each galaxy in the plane parallel approximation. We then compute the corresponding density field on a cubical region with 128^3 cells. This permits us to make efficient computations of the 2D power spectrum. We note however, that our ARGO code has been implemented to deal with non-parallel RSD. We obtain converged Gibbs-sampling chains after about 1000 iterations in terms of converged power spectra and also according to our convergence study demonstrated in (Ata et al. 2015). We have tested here different levels of deviation from Poissonity. As in Ata et al. (2015), we find that the stochastic bias can enhance the power towards high ks, however, this is not essential to our work. The smoothing scale r_S and the threshold δ_th can be tuned to compensate for that. Since we do not aim at getting the perfectly unbiased dark matter density field in this work, but to correct for RSD, we will show only results effectively sampling from the Poisson likelihood. An extension of this work investigating also the reconstructed dark matter field will be presented in Ata et al. (in preparation).

We run three reconstruction chains, two correcting only for coherent RSDs, and the third one correcting also (partially) for virialized RSDs. (i) The first RSD correction is based on coherent peculiar motions directly derived from the density field on a mesh using linear theory. (ii) The second one uses a smooth density field with Gaussian smoothing radius of $7\,h^{-1}$ Mpc obtained in a parameter study to optimally correct for RSD up to higher ks. (iii) The third one includes virialized corrections as described in Section 2.2.2.
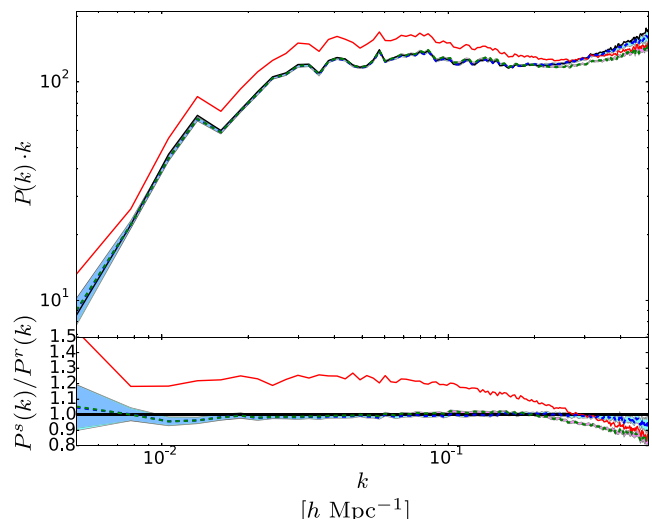

Figure 1. Upper panel: power spectra of the catalogue in redshift space (red), in real space (black); and of the reconstructed catalogues with only coherent flows (dashed green) with 1σ contour based on 1000 reconstructions (magenta), coherent flows including virialization corrections (dashed blue) with 1σ contour (cyan). Lower panel: ratio between the power spectra in redshift- $P^s(k)$ and in real-space $P^r(k)$ with the same colour code.

The resulting power spectra considering 1000 reconstructions only for the latter two cases for clarity are shown in Fig. 1. The first case yields a similar result on large scales, however underestimating the power in intermediate and small scales. Here we can clearly see that the Kaiser factor is corrected and that the non-linear RSD correction increases the clustering power towards small scales being closer to the true real-space catalogue. Fig. 2 shows the monopole and quadrupole in configuration space. We can see from these plots that the two different reconstructions: coherent with optimal smoothing or coherent and virialized motions corrections yield similar results. The left-hand panel shows how accurately the real-space baryon acoustic oscillations (BAO) can be obtained from redshift space. However the right choice of the smoothing scale is important here, or a non-linear virialized treatment to obtain a close BAO peak to the true one. We will quantify this improvement investigating also BAO reconstruction in a forthcoming work. Interestingly, the full non-linear RSD correction algorithm shows better agreement with the true real-space quadrupole not only on small scales being closer to zero, but also at large scales, displaying less artificial spikes, present in the pure coherent RSD corrections. However, the different quality in the reconstructions can be better appreciated in Fig. 3 showing the 2D power spectra. The anisotropic pattern in redshift space can be clearly seen. In particular, the enhancement of power due to the Kaiser effect is very prominent. A reconstruction of the peculiar velocity field with our method corrects the RSD in the catalogue in a remarkable way. We can see that an optimal choice of the smoothing scale can considerably improve the reconstruction. This is furthermore improved to scales of about $k \sim 0.3\,h\,\mathrm{Mpc^{-1}}$ when including virialized motions corrections.

4 SUMMARY AND DISCUSSION

We have presented in this work a Bayesian technique to correct for both coherent and virialized RSD present in galaxy catalogues by estimating the distance to the individual galaxies. We have
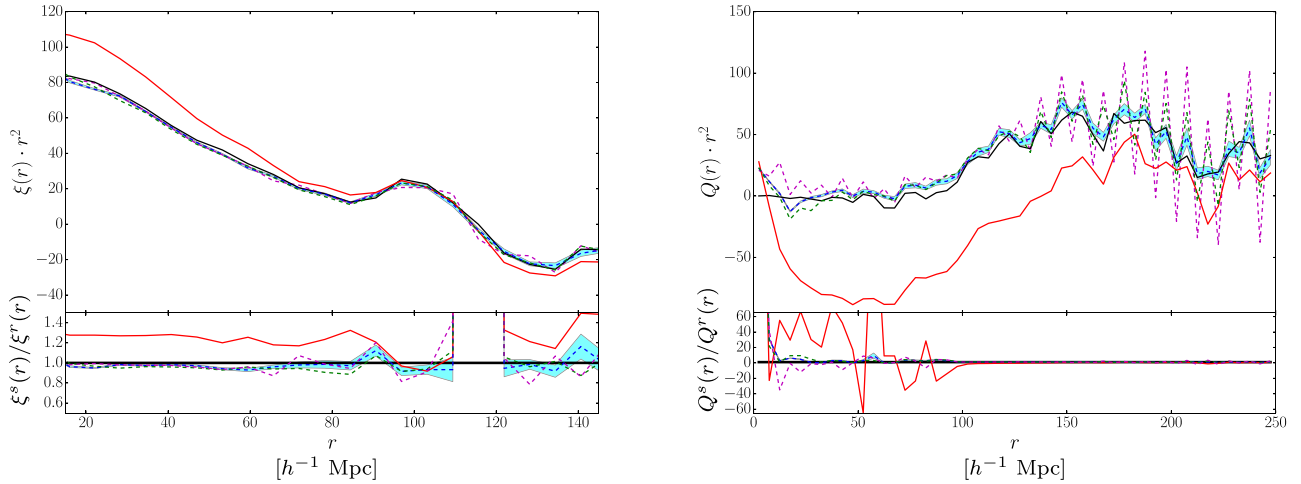
Figure 2. Left-hand panel: correlation function of the catalogue in redshift- $\xi^s(r)$ (red), in real space $\xi^r(r)$ (black); and of the reconstructed catalogues with coherent flows including virialization corrections (dashed blue) with 1σ contour of 20 samples (cyan). Additionally, the reconstructed catalogues with coherent flows corrections only are shown: magenta without Gaussian smoothing, green with optimal Gaussian smoothing of $r_S = 7\ h^{-1}$ Mpc. Right-hand panel: corresponding quadrupoles $Q^s(r)$, $Q^r(r)$. In the lower panels, the corresponding ratios with respect to the signal in real space are shown.
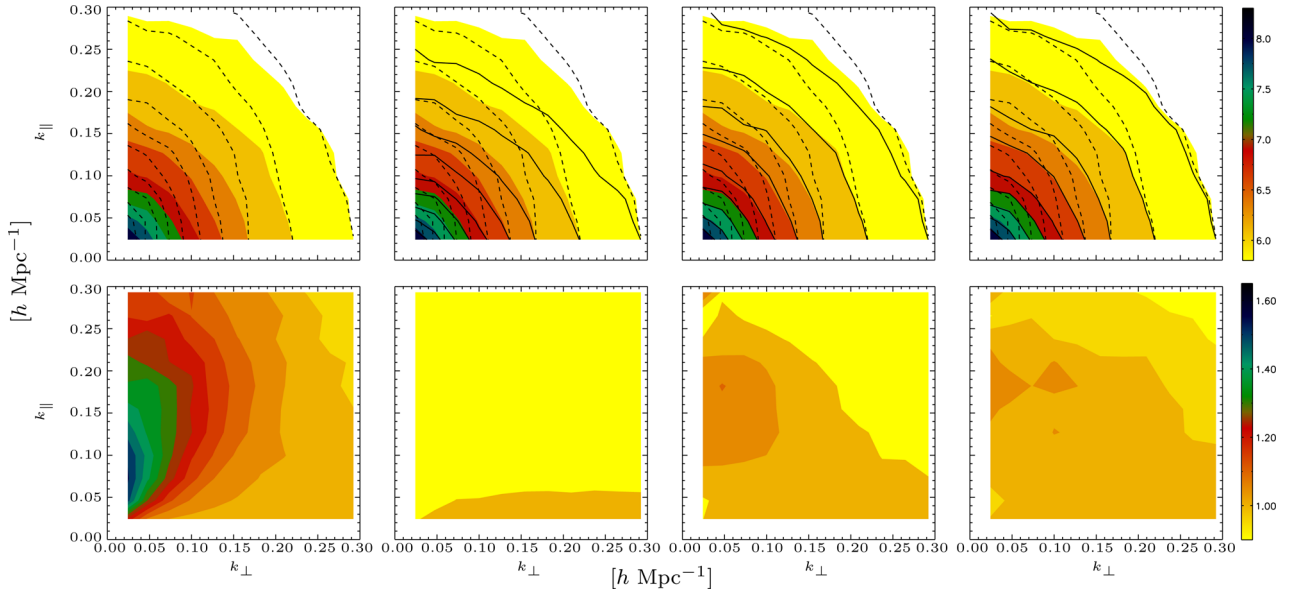
Figure 3. Upper panels: logarithm of 1+ the 2D power spectra $P(k_\perp, k_\parallel)$ corresponding to the mock galaxy catalogue in real space (colour-coded contour regions), in redshift space (dashed lines), including the reconstructed galaxy field in real space (solid lines): without any additional smoothing (second panel), with an optimal smoothing of $r_S = 7\ h^{-1}$ Mpc (third panel), including virialized RSD correction (fourth panel). Lower panels: corresponding ratio, (left-hand panel:) between the true catalogue in redshift- and in real-space, and (for the three panels on the right) between the corresponding reconstructed real-space catalogue and the true catalogue in real space.

demonstrated that this technique is accurate at least up to $k \sim 0.3\ h\ \mathrm{Mpc}^{-1}$ in the isotropization of the 2D power spectrum based on precise galaxy mock catalogues describing the CMASS LRG sample. The accuracy of this method towards smaller scales, also considering larger fractions of satellites than those present in LRG samples, remains to be investigated.

BAO reconstruction techniques do also deliver an estimate of the peculiar velocity field, being proportional to the displacement field in linear theory (see e.g. Eisenstein et al. 2007; Padmanabhan et al. 2012; Burden, Percival & Howlett 2015; Vargas-Magaña et al. 2015). These methods are equivalent to one-step linear solvers, which have been demonstrated to yield improved velocity estimates when extended to iterative approaches (e.g. Yahil et al. 1991; Wang

et al. 2012). While traditional RSD measurements focus on the growth rate, an approach like the one presented in this work is complementary and more general. We refer to a recent application of a joint analysis of density fields and anisotropic power spectra including growth rate estimation, see Granett et al. (2015). The advantage of the approach presented in the present work is that it deals with non-linear structure formation, non-linear and stochastic galaxy bias (Ata et al. 2015), including mask and selection treatments (Jasche & Kitaura 2010). It also yields, as a by-product, the real-space positions of the individual galaxies. The density fields can be used to obtain an improved displacement field less affected by shot noise than directly Gaussianizing the galaxy field (Falck et al. 2012; Kitaura & Angulo 2012).

An application of this technique to the BOSS DR12 data including power spectrum sampling will be presented in a subsequent publication (Ata et al. in preparation).

This technique is promising for a broad number of applications, such as correcting for photometric RSD including the cosmic web information, or to study the missing baryons problem (Planck Collaboration XXXVII 2015). We have demonstrated in particular that it is a potentially interesting technique for the estimation of the growth rate, or for an improved BAO reconstruction. These topics will be investigated in detail in forthcoming publications.

REFERENCES

Ata M., Kitaura F.-S., Müller V., 2015, MNRAS, 446, 4250
Bel J. et al., 2014, A&A, 563, A37
Berlind A. A., Narayanan V. K., Weinberg D. H., 2001, ApJ, 549, 688
Beutler F. et al., 2014, MNRAS, 443, 1065
Blake C. et al., 2011, MNRAS, 415, 2876
Blake C. et al., 2013, MNRAS, 436, 3089
Burden A., Percival W. J., Howlett C., 2015, MNRAS, 453, 456
Cole S., Fisher K. B., Weinberg D. H., 1995, MNRAS, 275, 515
da Ângela J. et al., 2008, MNRAS, 383, 565
de la Torre S. et al., 2013, A&A, 557, A54
Eisenstein D. J., Seo H.-J., Sirko E., Spergel D. N., 2007, ApJ, 664, 675
Falck B. L., Neyrinck M. C., Aragon-Calvo M. A., Lavaux G., Szalay A. S., 2012, ApJ, 745, 17
Granett B. R. et al., 2015, A&A, 583, A61
Guzzo L. et al., 2008, Nature, 451, 541
Hahn O., Porciani C., Carollo C. M., Dekel A., 2007, MNRAS, 375, 489
Hamilton A. J. S., 1998, in Hamilton D., ed., Astrophysics and Space Science Library Vol. 231, The Evolving Universe. Kluwer, Dordrecht, p. 185
Heß S., Kitaura F.-S., Gottlöber S., 2013, MNRAS, 435, 2065
Jackson J. C., 1972, MNRAS, 156, 1p
Jain B., Zhang P., 2008, Phys. Rev. D, 78, 063503
Jasche J., Kitaura F.-S., 2010, MNRAS, 407, 29
Jennings E., Baugh C. M., Pascoli S., 2011, MNRAS, 410, 2081
Kaiser N., 1987, MNRAS, 227, 1
Kitaura F.-S., 2012, MNRAS, 420, 2737
Kitaura F.-S., 2013, MNRAS, 429, L84
Kitaura F. S., Angulo R. E., 2012, MNRAS, 425, 2443

Kitaura F.-S., Enßlin T. A., 2008, MNRAS, 389, 497
Kitaura F.-S., Jasche J., Metcalf R. B., 2010, MNRAS, 403, 589
Kitaura F.-S., Gallerani S., Ferrara A., 2012a, MNRAS, 420, 61
Kitaura F.-S., Angulo R. E., Hoffman Y., Gottlöber S., 2012b, MNRAS, 425, 2422
Kitaura F.-S., Erdoğdu P., Nuza S. E., Khalatyan A., Angulo R. E., Hoffman Y., Gottlöber S., 2012c, MNRAS, 427, L35
Kitaura F.-S., Yepes G., Prada F., 2014, MNRAS, 439, L21
Kitaura F.-S., Gil-Marín H., Scóccola C. G., Chuang C.-H., Müller V., Yepes G., Prada F., 2015, MNRAS, 450, 1836
Klypin A., Yepes G., Gottlober S., Prada F., Hess S., 2014, preprint (arXiv:1411.4001)
Kwan J., Lewis G. F., Linder E. V., 2012, ApJ, 748, 78
McDonald P., Seljak U., 2009, J. Cosmol. Astropart. Phys., 10, 7
Nesseris S., Perivolaropoulos L., 2008, Phys. Rev. D, 77, 023504
Neyrinck M. C., Szapudi I., Szalay A. S., 2009, ApJ, 698, L90
Nuza S. E., Kitaura F.-S., Heß S., Libeskind N. I., Müller V., 2014, MNRAS, 445, 988
Okumura T., Matsubara T., Eisenstein D. J., Kayo I., Hikage C., Szalay A. S., Schneider D. P., 2008, ApJ, 676, 889
Okumura T., Seljak U., Desjacques V., 2012, J. Cosmol. Astropart. Phys., 11, 14
Okumura T., Seljak U., Vlah Z., Desjacques V., 2014, J. Cosmol. Astropart. Phys., 5, 3
Padmanabhan N., Xu X., Eisenstein D. J., Scalzo R., Cuesta A. J., Mehta K. T., Kazin E., 2012, MNRAS, 427, 2132
Peacock J. A. et al., 2001, Nature, 410, 169
Percival W. J., White M., 2009, MNRAS, 393, 297
Percival W. J. et al., 2004, MNRAS, 353, 1201
Planck Collaboration XXXVII 2015, preprint (arXiv:1504.03339)
Reid B. A. et al., 2012, MNRAS, 426, 2719
Reid B. A., Seo H.-J., Leauthaud A., Tinker J. L., White M., 2014, MNRAS, 444, 476
Samushia L., Percival W. J., Raccanelli A., 2012, MNRAS, 420, 2102
Samushia L. et al., 2013, MNRAS, 429, 1514
Samushia L. et al., 2014, MNRAS, 439, 3504
Sánchez A. G. et al., 2014, MNRAS, 440, 2692
Song Y.-S., Koyama K., 2009, J. Cosmol. Astropart. Phys., 1, 48
Song Y.-S., Percival W. J., 2009, J. Cosmol. Astropart. Phys., 10, 4
Song Y.-S., Sabiu C. G., Nichol R. C., Miller C. J., 2010, J. Cosmol. Astropart. Phys., 1, 25
Song Y.-S., Sabiu C. G., Kayo I., Nichol R. C., 2011, J. Cosmol. Astropart. Phys., 5, 20
Springel V., 2005, MNRAS, 364, 1105
Tojeiro R. et al., 2014, MNRAS, 440, 2222
Vargas-Magaña M., Ho S., Fromenteau S., Cuesta A. J., 2015, preprint (arXiv:1509.06384)
Wang H., Mo H. J., Yang X., van den Bosch F. C., 2012, MNRAS, 420, 1809
White M., Song Y.-S., Percival W. J., 2009, MNRAS, 397, 1348
Yahil A., Strauss M. A., Davis M., Huchra J. P., 1991, ApJ, 372, 380
Zhang P., Liguori M., Bean R., Dodelson S., 2007, Phys. Rev. Lett., 99, 141302
Zhao G.-B., Giannantonio T., Pogosian L., Silvestri A., Bacon D. J., Koyama K., Nichol R. C., Song Y.-S., 2010, Phys. Rev. D, 81, 103510
Zhao C., Kitaura F.-S., Chuang C.-H., Prada F., Yepes G., Tao C., 2015, MNRAS, 451, 4266
Zheng Y., Zhang P., Jing Y., Lin W., Pan J., 2013, Phys. Rev. D, 88, 103510

This paper has been typeset from a TEX/LATEX file prepared by the author.